Level-1 sTGC Trigger Studies for the ATLAS New Small Wheel Upgrade

Jennifer Roloff
Advisor: Junjie Zhu
The University of Michigan

1 Introduction to the Standard Model, CERN, and the LHC

1.1 The Standard Model

The Standard Model (SM) is a model describing fundamental particles and their interactions. In this theory, there are two classes of fundamental particles: fermions and bosons. Fermions are spin-1/2 particles and include electrons, muons, taus, their corresponding neutrinos, and six quarks (up, down,strange, charm, top, and bottom). These particles all have corresponding antiparticles, and each quark flavor can have one of three different colors. There are four types of interactions which these particles experience, named the strong, weak, electromagnetic, and gravitational forces. These forces, with the exception of gravity, are mediated by spin-1 bosons. The force carrier is the photon for the electromagnetic force, the gluon for the strong force, and the W and Z bosons for the weak force [5].

Although this theory fits experimental results to high accuracy, there are still phenomena that it fails to explain. For instance, gravity is not explained in the SM, nor is the amount of Dark Matter. Physicists hope to explore new physics beyond the SM, hopefully leading to a more unified and comprehensive theory of physics. The topics that particle physicists are currently studying include the source of electroweak symmetry breaking mechanism, the existence of new fundamental symmetries, extra force carriers, fermions, and spacial dimensions, the properties of dark matter, and the source of matter-antimatter asymmetry. Particle colliders are the tools for studying the SM, since they are able to probe small scales using high energies [5].

1.2 CERN

The European Organization for Nuclear Research (CERN) was established in 1954, and is on the forefront of high energy physics research. It was founded in order to make Europe competitive in Nuclear Physics (CERN's early history revisited) after World War II. As the energy frontier increased, scientists at CERN continued research on the forefront of high energy physics by building increasingly large detectors. CERN first discovered the neutral current as well as the W and Z bosons. Most recently, the Large Hadron Collider (LHC) was built over the period 1998 to 2008 to collide particles at record energies. The LHC houses six experiments: ATLAS, CMS, LHCb, ALICE, TOTEM, and LHCf.

1.3 The LHC

With a 27 km circumference, the LHC is the world's highest energy particle collider, built to collide protons with energies of up to 14 TeV per collision. Colliders and detectors combine to smash particles together at high energies and see what particles are produced. Using Einstein's equation $E = mc^2$, mass and energy can be exchanged. Defining $s = (p_1 + p_2)^2$, where p_1 and p_2 are the 4-momenta of the colliding particles, we find that in the center-of-mass frame, $E_{CM} = \sqrt{s}$. This energy relates to the maximum mass that a created particle may have. Thus, higher energy colliders allow a wider variety of particles to be created in collisions [5], [3].

There are several ways of measuring the performance of a collider. First, there is the beam energy, also called the center-of-mass energy. Higher energy means that inelastic events will occur more frequently. The likelihood of the collision having enough energy to break apart the proton

increases, and particles with higher energies may be created more frequently. Another measure of the performance is the instantaneous luminosity, or how many particles per area pass through each other. The instantaneous luminosity is proportional to fn_1n_2/a, where f is the beam crossing frequency, a is the transverse profile of the beam, and n_1 and n_2 are the particles in colliding beams 1 and 2. Defined as such, the instantaneous luminosity is proportional to the rate of collisions. The instantaneous luminosity has a unit of $\text{cm}^{-2}\ \text{s}^{-1}$. Higher integrated luminosity gives more statistics, giving more sensitivity to new physics [3].

The LHC has two proton beam lines, which collide at several points along the accelerator ring at a collision rate of 40 MHz. Protons are composed of many partons, including quarks, gluons, and antiquarks, and in high energy collisions, such as those at the LHC, it is these partons that interact, not the protons as a whole. Compared to lepton accelerators, pp colliders have the benefit of being able to attain higher energies in a circular collider because they have less synchrotron radiation [3]. Proton accelerators are also able to probe a wide range of the energy domain since individual partons carry different fractions of the total energy of the proton.

Since being turned on in 2009, the LHC has been ramping up its energy, running at 7 TeV in 2011, 8 TeV in 2012, and after the current upgrade, the energy will most likely be raised to 13 TeV with the ultimate goal of 14 TeV. From 2010-2012, the instantaneous luminosity has increased from 10^{27} to $6\times10^{34}\ \text{cm}^{-2}\ \text{s}^{-1}$. The total integrated luminosity is 5 fb^{-1} at 7 TeV and 21 fb^{-1} at 8 TeV. Plans are underway to upgrade the LHC to allow it to operate at higher energy and luminosity. The instantaneous luminosity is expected to be $2-5\times10^{34}\ \text{cm}^{-2}\ \text{s}^{-1}$ after the phase I and II upgrades, and the total integrated luminosity is expected to be 300-3000 fb^{-1} [2].

2 ATLAS

2.1 The ATLAS Detector

With a size of 46 m $\times$ 25 m $\times$ 25 m, weighing 7000 tonnes, and involving around 3,000 physicists, ATLAS, A Toroidal LHC ApparatuS, is one of the largest experiments at CERN [1]. It is an general-purpose detector, studying a broad range of topics on the forefront of high-energy physics research. Particle detectors work much like cameras, recording "images" of each collision that occurs. Most of the particles that these experiments search for have short lifetimes and decay quickly, meaning that they cannot be detected directly. Instead, ATLAS detects the final state particles in order to reconstruct the original particle. In order to search for a broad range of phenomenon, ATLAS has been designed to measure various physics objects such as leptons, photons, jets, and missing transverse energy (MET) accurately. This allows us to detect the signatures of the different decays, and measure how high above background they are, determining whether we have "seen" a specific particle. [2]

Particle detectors work on the principle that different classes of particles interact with detector materials differently, making the task of detecting particles simpler. In ATLAS, different subdetector systems are used to identify and track different particles. Other particles, such as neutrinos, interact very little with the detectors because of their small cross section with material, and must be found indirectly using missing transverse energy (MET). Although the product of collisions is widely varied, energy and momentum must be conserved. For head-on collisions, the initial total momentum on the transverse plane (the plane perpendicular to the beam line) is zero. Consequently,

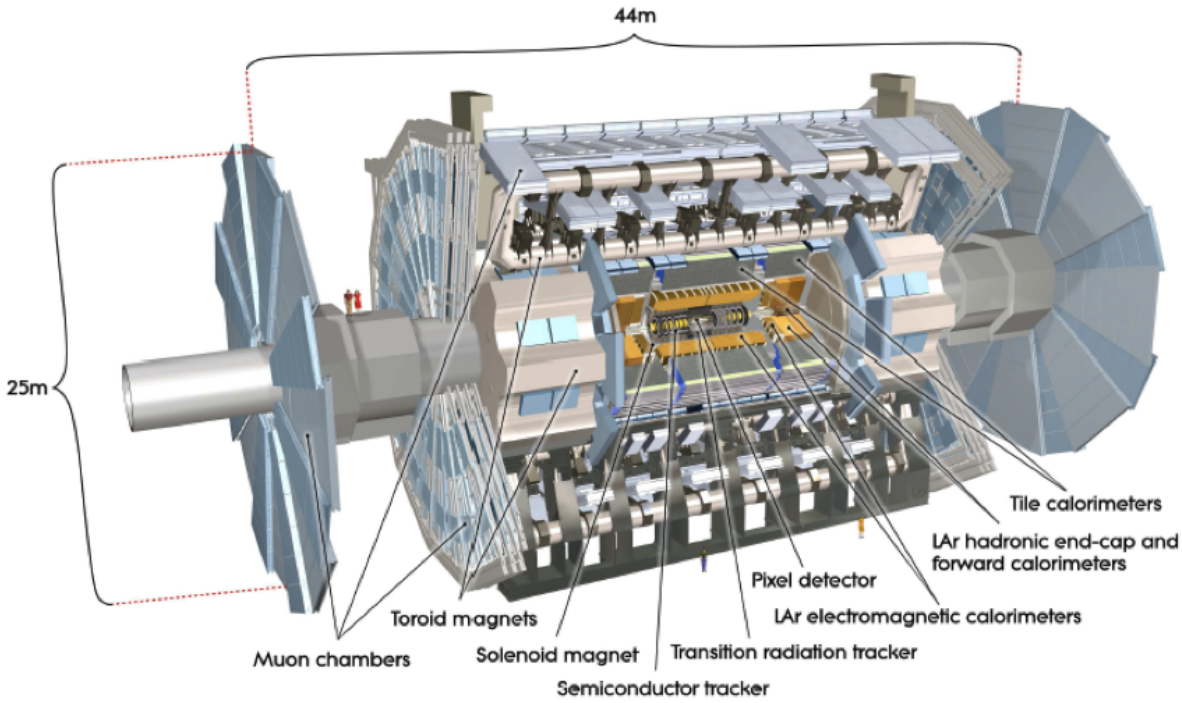

Figure 1: The ATLAS detector [4]

the sum over the transverse momenta of the all final particles must also be zero. The neutrino p_x and p_y can be added to the detected p_x and p_y to make the total momentum zero.

A general layout of the detector is shown in Fig. 1. The innermost detector is the tracking chamber, which measures the momentum and direction of charged particles inside the magnetic field and uses this to determine the location of the primary collision position. The innermost layer, the Inner Detector, helps determine particle type and momentum, and helps determine the origin of the particle. It is composed of a pixel detector, semi-conductor tracker (SCT), and a Transition Radiation Tracker (TRT). By measuring the curvature of tracks from the magnetic field, the charge and momentum of the particle may be determined. The pixel detector has over 80 million readout channels, which are able to give precise information on particle position. The SCT has fewer channels than the pixel detector, but is crucial to tracking since it covers a larger area. When passing between materials with different indices of refraction, particles produce transition radiation which can be detected by the TRT. The amount of radiation varies based on the speed and mass of the particles, allowing for particle tracking and identification. The TRT is particularly useful in distinguishing between electrons and photons [2].

Next, the electromagnetic calorimeter primarily measures electron and photon energy, while the hadron calorimeter detects hadrons. The particles will create showers while passing through the detectors, and the deposited energy from these showers can be detected. The calorimeter is composed of a Liquid Argon (LAr) system and a Hadronic Calorimeter. This layer of detectors serves to absorb most of the particles, with the exception of muons, and in the process measure the energy deposits. The LAr system measures and absorbs particles that interact electromagnetically. In the process, it measures the particle's trajectory and pseudorapidity (η). The Hadronic Calorimeter

absorbs particles that interact via the strong force. [2]

Finally, the outermost detector, the muon spectrometer, detects the muons, since in principle all other charged particles should be stopped in the calorimeter. It surrounds the calorimeter and is composed of Monitored Drift Tubes (MDTs) and Cathode Strip Chambers (CSCs) as precision tracking chambers, and Resistive Plate Chambers (RPCs) and Thin Gap Chambers (TGCs) as trigger chambers [2].

ATLAS has two types of magnets which bend the paths of the outgoing particles: a thin solenoid around the inner tracking system and barrel and endcap toroid magnets which affects the z-coordinate of particles. These allow detectors to measure the momentum and charge of particles [2].

3 The ATLAS Trigger

One final complication of high energy experiments is the data collection rate. Every 25 ns, there is one bunch crossing at the LHC. Were all the data from these collisions recorded, it would fill nearly 100,000 CDs per second. [1] It is impossible to store all of this data, so alternatives must be sought, in this case, triggering. Triggers separate important events from those that may be discarded without ignoring important new physics. Since the LHC has such a high luminosity, generating around 40 million events per second, it is necessary to filter through the events since only a limited amount of data may be stored. In order to create an effective trigger, we must search for specific signatures of important events. For instance, many interesting physics processes produce high p_T muons, so one can trigger on events with high p_T muons. However, triggers are not limited to this. Triggers can be based on particle type, number of that type of particle, kinematics, event topology, and other things [2].

There are several levels of triggering at ATLAS. The Level-1 trigger uses the muon spectrometer and calorimeter to determine the transverse momentum (p_T) of the particle. The Level-1 trigger is mainly hardware based and screens particles using a very basic algorithm, which outputs events at a rate of 75 kHz. Since this is done in-time and looks at all events, it must filter events quickly, and so only the most basic algorithms are used. The Level-2 trigger has a little more time, and after a mixture of hardware and software, it only looks at events that pass the Level-1 trigger, so it can do some simple reconstruction to analyze events better. Finally, offline reconstruction is done with the events that pass the Level-2 trigger to fully reconstruct events, including particle ID, each particle's p_T, particle path, among other things. The L2 trigger output rate is close to 10 kHz, and the event filter lowers this to around 700 Hz, which is what is ultimately recorded on the disk [2].

4 Motivation for ATLAS NSW Upgrade

4.1 The ATLAS Forward Muon Trigger

Figure 2 shows the layout of the ATLAS muon spectrometer. For the forward region, we have three MDT stations: the Small Wheel (SW), Big Wheel (BW), and Outer Wheel (OW) (located at $z = \pm 21$ m is not shown in this figure). There are magnets between the small and big wheels, which allows us to determine the muon transverse momentum by measuring the amount of bending.

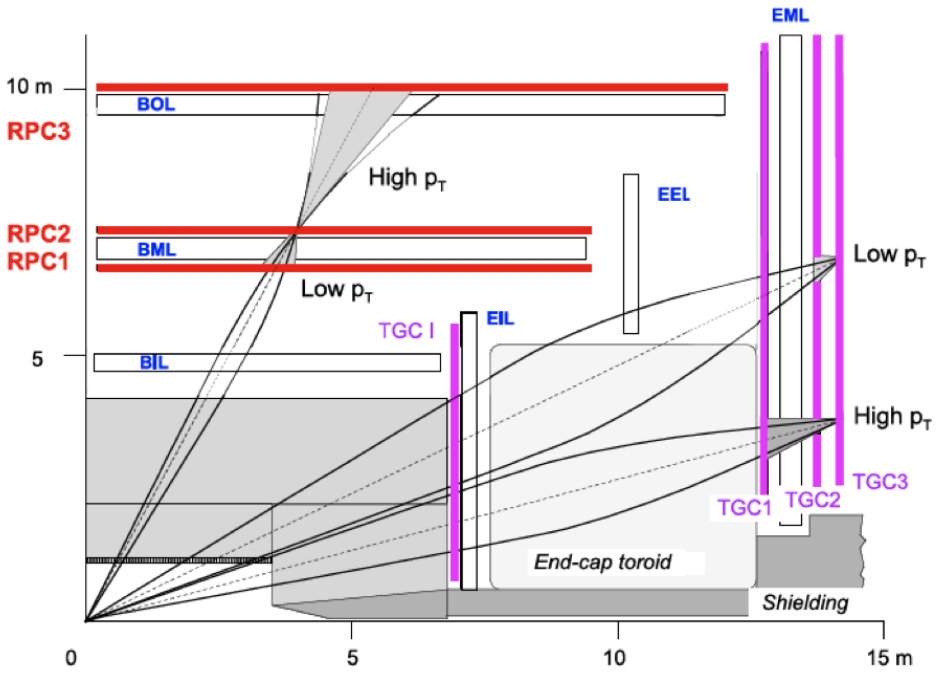

Figure 2: The ATLAS muon spectrometer and L1 trigger schematics [2]

The current L1 muon triggers only depend on the TGC chambers in the Big Wheel. The trigger algorithm determines the L1 muon p_T by measuring the deviation of the muon hit position from the expected unbent position. This algorithm assumes that all muons come from the origin.

4.2 The L1MU20 Trigger

Many interesting physics processes involve high p_T muons in the final state. It is important to record all of these events, not a randomly selected fraction of the events (called a pre-scale). One important trigger is the L1MU20 trigger, which selects events that have a muon with $p_T \geq 20$ GeV. Studies have shown that approximately 30% of L1MU20 events do not contain real muons, since they do not have reconstructed segments in the SW, and the rate of true high p_T tracks is only about 2% of the L1MU20 rate in the endcap. There are a couple reasons for this inefficiency. The L1MU20 events that do not correspond to a segment most likely occur by slow-momentum neutrons. Figure 4 shows how each level of triggers progressively eliminates more fake muons.

As the luminosity and beam energy increase after the 2013/2014 shutdown, the detectors and triggers must be more efficient in order to accommodate the increasing amount of data. As the instantaneous luminosity increases, so does the Level-1 muon trigger rate. Because of limited computing power which determines the rate of data storage, currently around 100 kHz at Level-1, this rate must be capped. However, with the present settings of the ATLAS forward muon trigger system, more than 90% of the muons triggered at L1 were due to cavern backgrounds, thus the endcap L1 muon trigger rate will exceed the maximum storage rate allocated for the whole muon system (20 kHz) when the instantaneous luminosity is increased to 3×10^{34} cm$^{-2}s^{-1}$.

In order to solve the L1 muon trigger rate problem at high energy and high luminosity LHC

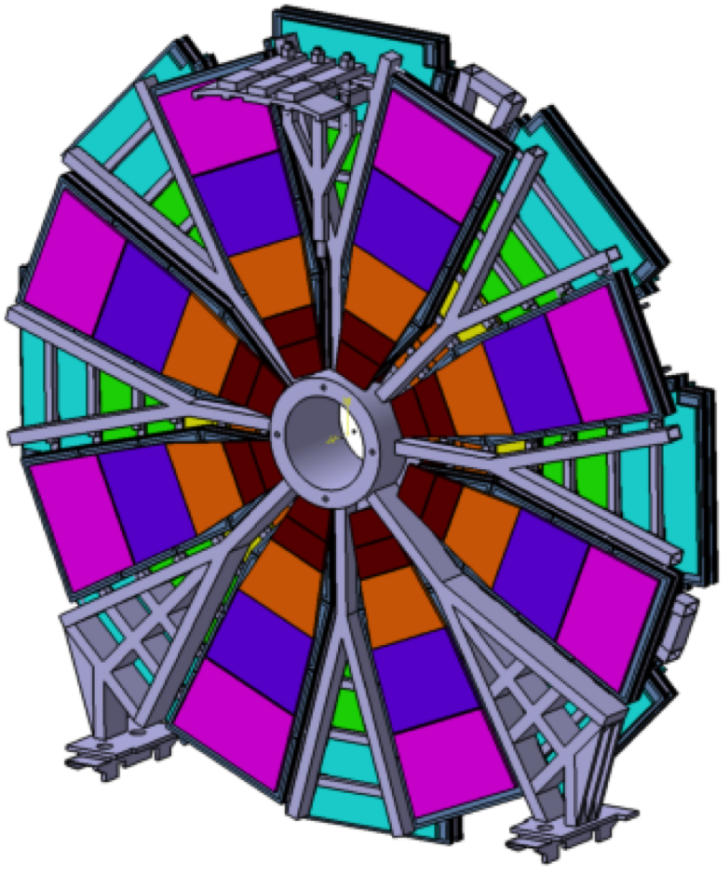

Figure 3: The proposed NSW detector. There are 8 small sectors and 8 large sectors for each wheel. [2]

runs, ATLAS plans to replace the current SW with a NSW detector. Additionally, precision tracking detectors like MDTs and CSCs degrade under the increased radiation and thus the offline muon reconstruction efficiency and the momentum measurement will drop significantly, meaning that they must either be replaced or shielded more effectively. For the trigger upgrade, this NSW detector will provide segments measurements which can be matched to segments found by the TGC detectors in the BW. This should reduce the L1MU20 rate to 15% of its original value. However, even if we remove all fake muons, only 10% of L1MU20 events contain muons with $p_T \geq 20$ GeV since many lower p_T muons are misidentified as having $p_T > 20GeV$ at L1 due to low p_T resolution. The L1 p_T resolution is related to several factors, including the TGC station angular resolution, multiple scattering in the endcap toroid and calorimeters, and the finite size of the pp collision region. The current L1 p_T resolution is about 30% for 20 GeV muons. If we can have a precise measurement of the muon angular direction in the SW region, we can use the angular difference for the muon segments in the BW and SW to determine the muon p_T more precisely.

There are several requirements for the NSW regarding the rate capabilities, aging characteristics, performance, and triggering capabilities. There are two goals for the upgraded detector. First, it must be able to withstand rates up to $10-14$ kHz/cm^2. Secondly, the NSW segments at L1 must have an angular resolution of at least 1 mrad.

ATLAS decided to use 8 layers of micromega detectors for precision tracking and 8 layers of

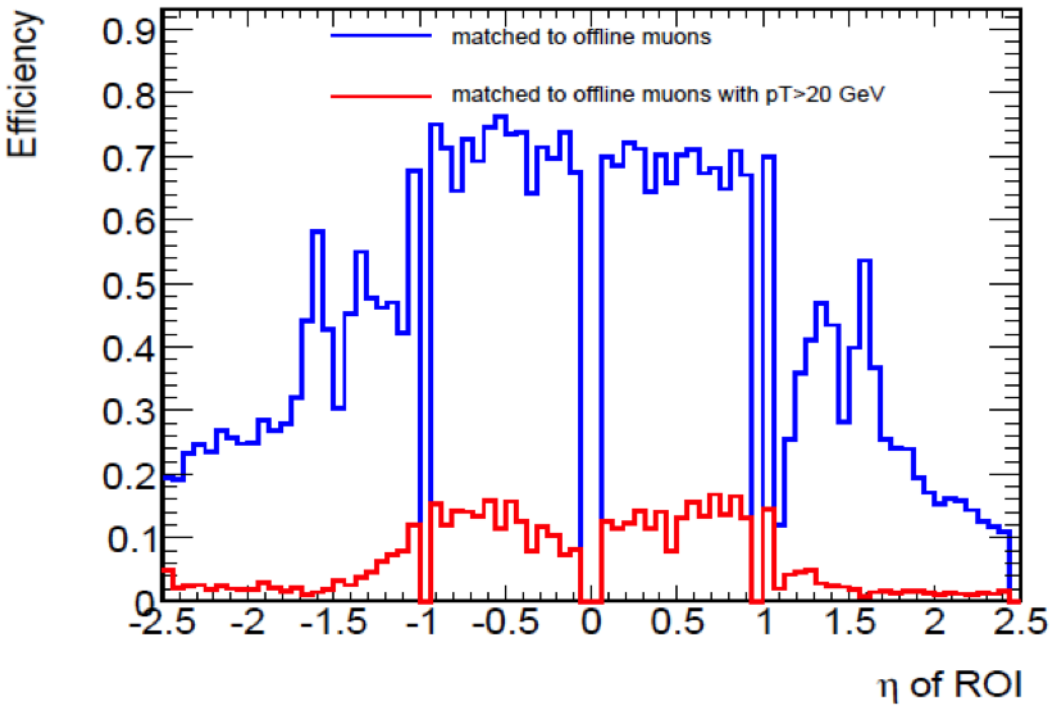

Figure 4: The efficiency of matching L1 events to events passing the L2 and offline triggers

super TGC (sTGC) detectors for triggering. These 8 sTGCs will be divided between two stations of TGCs and are separated by 36 cm with the micromegas. Each layer will have 8 small sectors and 8 large sectors with four sTGC chambers per sector. This layout can be seen in Fig. 3. sTGCs are a good choice of detector for the increased luminosity since they have a fast response time and do not noticeably degrade after large amounts of radiation. Also, they have been effective in the current ATLAS detector, making it an easier transition to the new system.

5 sTGCs studies in the NSW

5.1 sTGCs

The NSW detector will use sTGC detectors that can cope with the expected high instantaneous luminosity after the Phase-I upgrade. Compared with the present TGC detector, the new detector will be modified including the distance between the readout strips and the graphite layer, the surface resistivity of the graphite layer, the size of the readout strip pitch and the addition of pad triggers. The rate capability can be improved by placing the strip readout as close as possible to the graphite layer (e.g. 100 μm). Such configuration would allow reducing the surface resistivity from the present 1 MΩ/square to 10-20 kΩ/square while keeping the same transparency on the graphite cathodes. The readout strip pitch size will be reduced from 2 cm to about 3 mm to achieve a spatial resolution of 100 μ m. Pad triggers are needed to reduce number of strips to be considered at L1.

The SW sTGC trigger will look for coincidence in 6 of 8 pads, where each pad has a size of about 8 cm by 8 cm. These fired pads will provide the list of strip bands to be read out. The signals

from the sTGC strips will be amplified, shaped, and discriminated to determine the deposited charge information. This data will be used to determine the centroid for the layer, and the centroids from each of the four layers will determine the average position for each station. Centroids from two stations will be fit with a line to determine the muon direction in the SW, which can be used to calculate the deflection angle and p_T.

5.2 sTGC Spatial Resolution

sTGCs in the NSW will provide high quality segment measurement, reduce the fake rate, and improve the p_T resolution. It is important to make sure that these sTGC chambers satisfy the basic upgrade requirements. Several beam tests have been conducted to study sTGC performance at CERN's SPS test beam facility. To calculate the resolution, events were selected with a parallel beam. Only events where hits are at least two strips from the edge of the detector were used. Information on the Time-over-Threshold (TOT) gives a fast estimation of the charge. The TOT information for each strip was fitted with a Gaussian, giving a resolution of residual between two neighbor layers / $\sqrt{2}$ or plotting the residual of the 8th layer after fitting the first 7. The resolution was measured at several angles of incident radiation, giving a range of 86 μm at 0 degrees to 169 μm at 30 degrees. The spatial resolution is found to be between 90 and 170 μm, with dependence on the incident angle. With a level arm of 36 cm and 8 independent measurements, this will satisfy the 1 mrad angular resolution requirement. On average, 96% of events fall within a 25 ns time window, showing the need for more improvements.

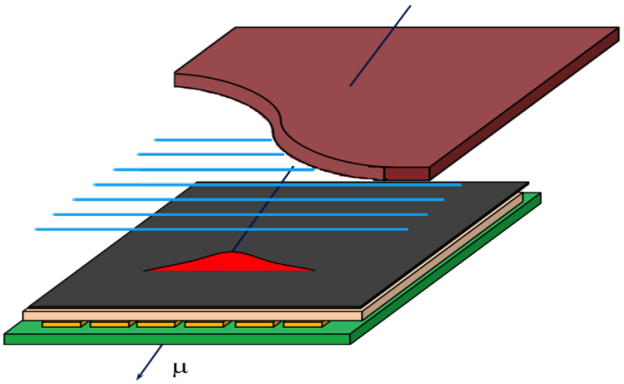

Figure 5: sTGC structure

The structure of an sTGC detector is shwon in Figure 5. They are gaseous detectors, with operating gas 55% CO_2 + 45% N-pentane. They have 2.7 mm readout strips with a pitch size of 3.2 mm. Inside, they have wires separated by 1.8 mm, with 1.4 mm separation on either side from the walls of the chambers. Around 2.9 kV of high voltage is applied to the chambers.

In order to test the viability of the proposed upgrade of the sTGCs in the NSW, we have done several studies using single muon events from GEANT simulations. Knowing the location of the detectors, we were able to estimate the resolution using single muon events generated with fixed energy. The R and z-coordinates of the hits is shown in Figure 10. This clearly shows the structure of the detector, with the four sectors at different z-coordinates, and the four layers of detectors within each sector.

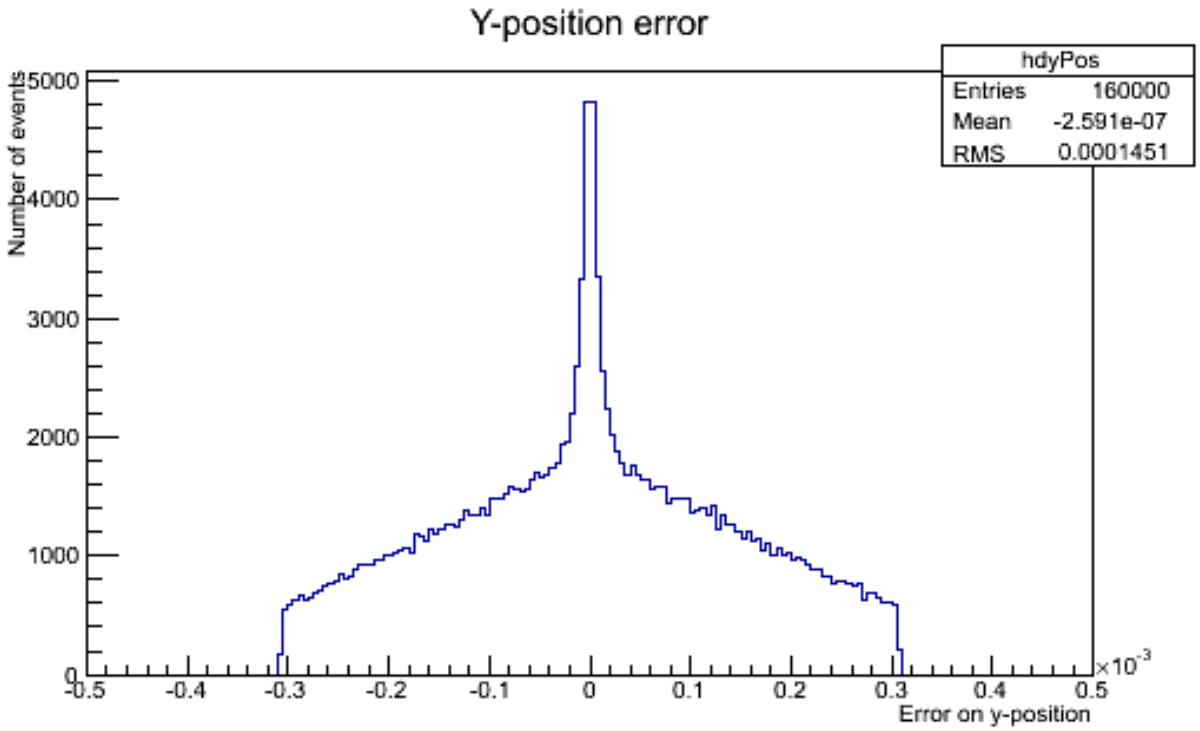

Figure 6: Spatial resolution of y-pos detector hits

The sTGC resolution was measured by the distance from the reconstructed hit location to the real hit location. The muon signal was modelled as a Gaussian with a variable width so that it deposits charge on several strips of the sTGC detector. The shower width was generated randomly using a Gaussian distibution with mean shower width of 3.335 mm with a standard deviation of .487 mm, the values obtained from the test beam measurements. Then, using strips of width 2.7 mm and pitch 3.2 mm, all the strips with at least 5% of the total charge were fitted with a Gaussian to determine the modelled hit location. A plot of the error on the reconstructed hit location is shown in Figure 6. Figure 7 shows the percentage of total charge that the strips detect. If all of the charge were detected, the reconstruction would be perfect, but the gaps between strips adds error. Additionally, the electronics add 6% noise, which is accounted for in the simulation by random fluctuation. An example of this fitting is shown in Figure 8. These show a resolution of 140 μm, consistent with the test beam results showing resolution of around 150 μm, as seen in Figure 9.

5.3 Pattern Recognition

Particles passing through the detectors will occasionally knock off other particles, leaving multiple tracks in the detector. In these cases, it is important to quickly determine which path corresponds to the original muon. In order to differentiate between different particle tracks, we created a pattern recognition algorithm which can determine hits belonging to the muon track. The following pattern recognition algorithm was employed. We looked at hits from the large and small sectors separately, where the small sector was composed of the two closest sectors (in z) and the large sector was composed of the farthest two sectors. First, all combinations of hits in the first and eighth (first

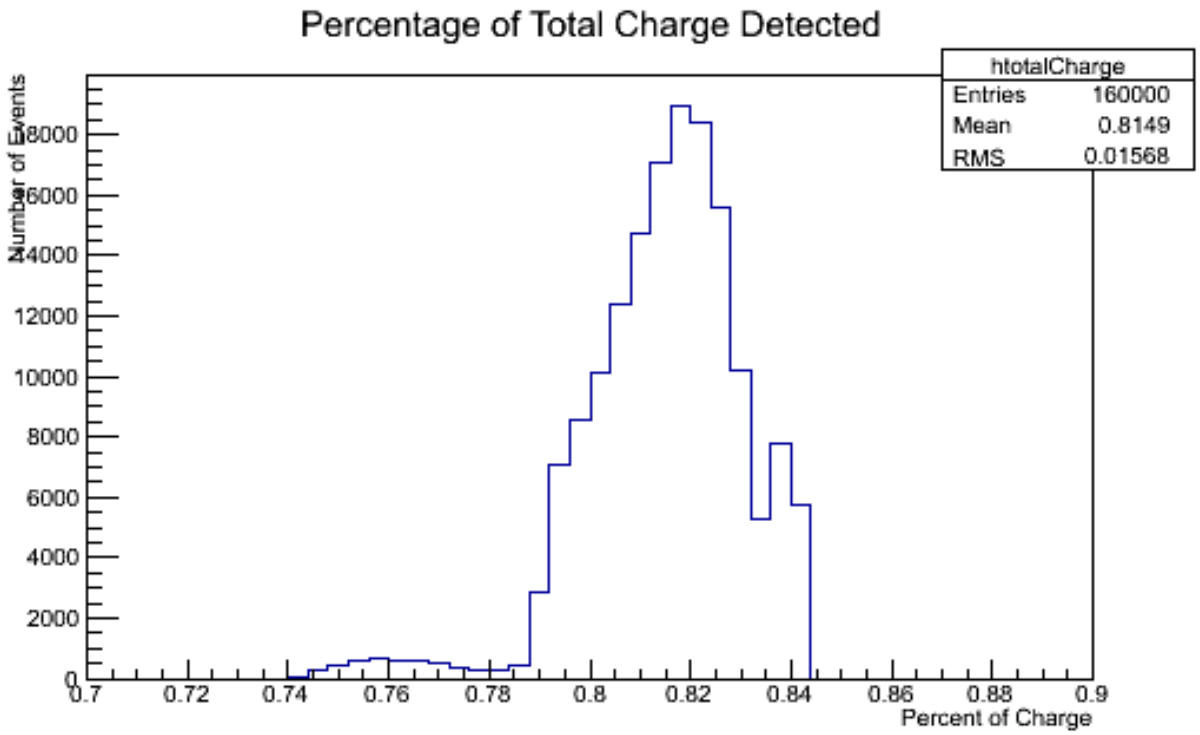

Figure 7: Distribution of total charge detected by a single hit

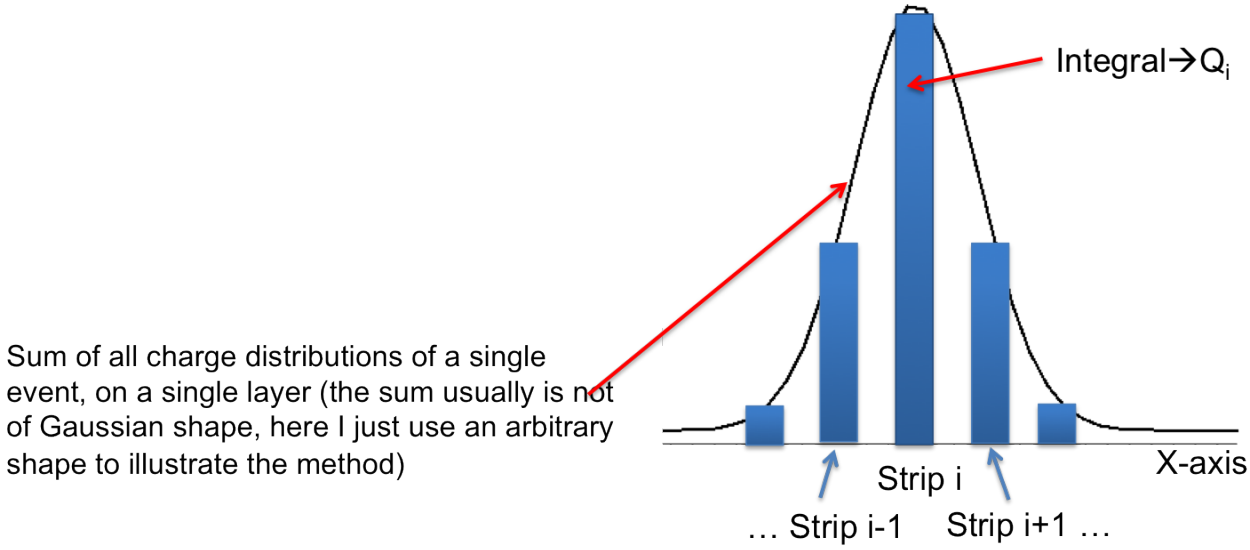

Figure 8: Example fitting of Gaussian using strips. The Gaussian shows the charge distribution, while the bars show the detector strips.

and last) detectors within either the large or small sectors were fitted with a line. These lines were traced back to the z-axis, and the intercept closest to the origin dictated the best path. Then, the other hits from the particle were hits that were within 3 sigma of the single hit resolution. Several examples of these hit patterns are shown in Figure 13.

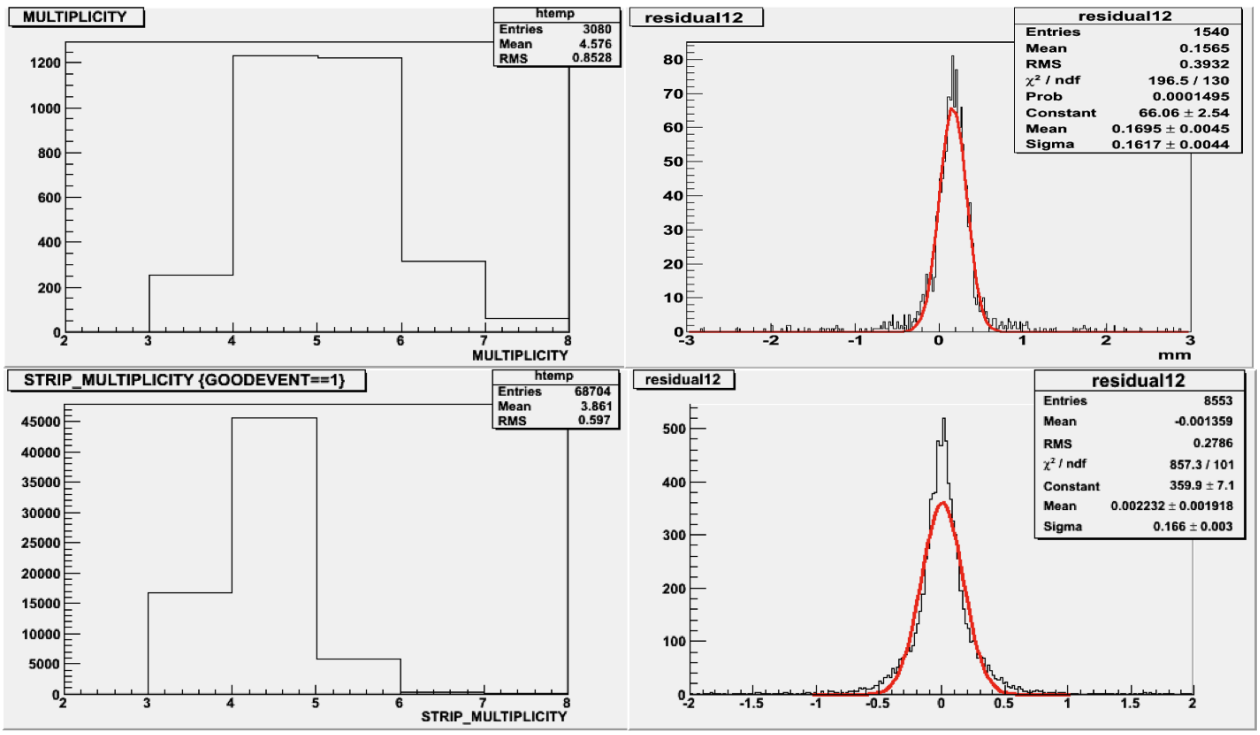

Figure 9: Comparison of data and simulation sTGC detectors for the strip multiplicity and spatial hit resolution. The top to plots are from test beam data, and the bottom two are from the GEANT simulation

To study muon paths we used 10,000 single muon events passed through the ATLAS GEANT simulation (no digitization simulation was ready at this time), where each hit was smeared by 150 μm. We first looked at only events with exactly 8 hits. Since there are 8 layers of detectors, each with a fairly high efficiency, most of these hits were from the muon path we wished to study. The hits were smeared by a gaussian with a mean value of 0 and a standard deviation of 150 μm. We looked at a number of these events to check that this matched our prediction, and all of the ones we looked at were indeed 8 hits from a single particle. From this, we were able to determine the variation from a line that these hits exhibited. We fit all 8 hits to a line, using a least squares algorithm, and then we plotted the difference in the hit location to the predicted position from the fitted line. This plot can be seen in Figure 12. The standard deviation of this distribution is 210 μm. This is slightly larger than the 150 μm due to the fact that we do not account for the magnetic field effects.

To see the accuracy of the pattern recognition algorithm, we looked at several parameters. First, we looked at how many hits were generally accepted. As seen in Figure 14, 57% of events had 8 hits. Since the sectors overlap slightly, some events had more than 8 hits. Some events had fewer than 8 hits, corresponding to events with hits smeared far from their origin, detectors that did not fire, and misreconstructed events. We also looked at the difference between the estimated and truth origins of the muon. As seen in Figure 15, most of them are within 18 mm of the real origin, though some are as far away as 60 mm. The combination of these results indicates that our algorithm is successful at identifying the correct particle path. Additionally, looking at the deviation of points from the reconstructed line as seen in Figure 17, the standard deviation is 240 μm, consistent with

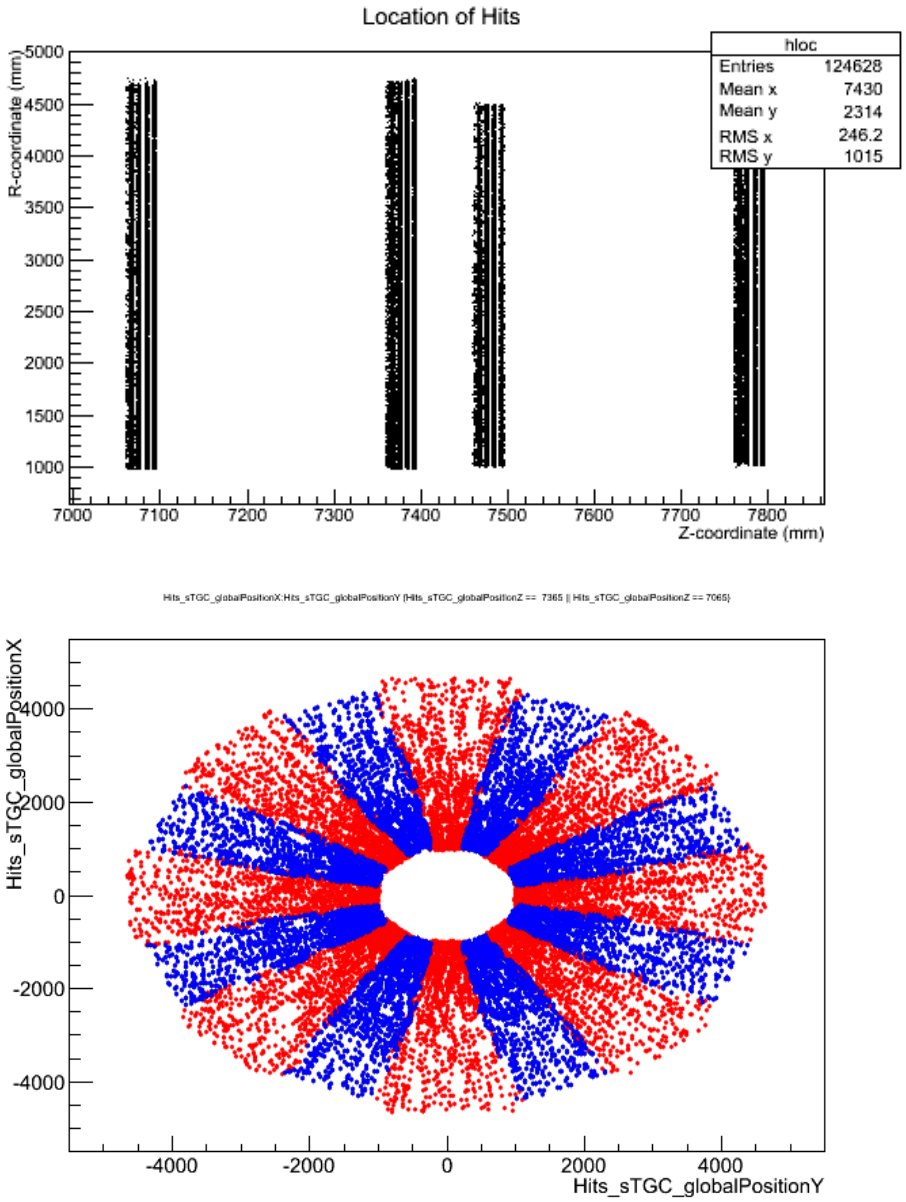

Figure 10: Hit Location in *r*-*Z* and *XY* coordinates. Figure b shows the hits from the 8 sectors closest to the origin in red, and the 8 farthest in blue.

the result from events with only muon hits.

5.4 Segment Angular Resolution

For particle paths, the efficiency was the probability that a particle would create a path that would be reconstructed. The resolution was determined by a couple factors, including the resolution of the origin as well as the angular resolution. To determine the efficiency and resolution, we used the individual TGC modelling to calculate the hit location for each detector along the muon's path. These points were fitted with a least squares algorithm, and that inclination of the line was compared

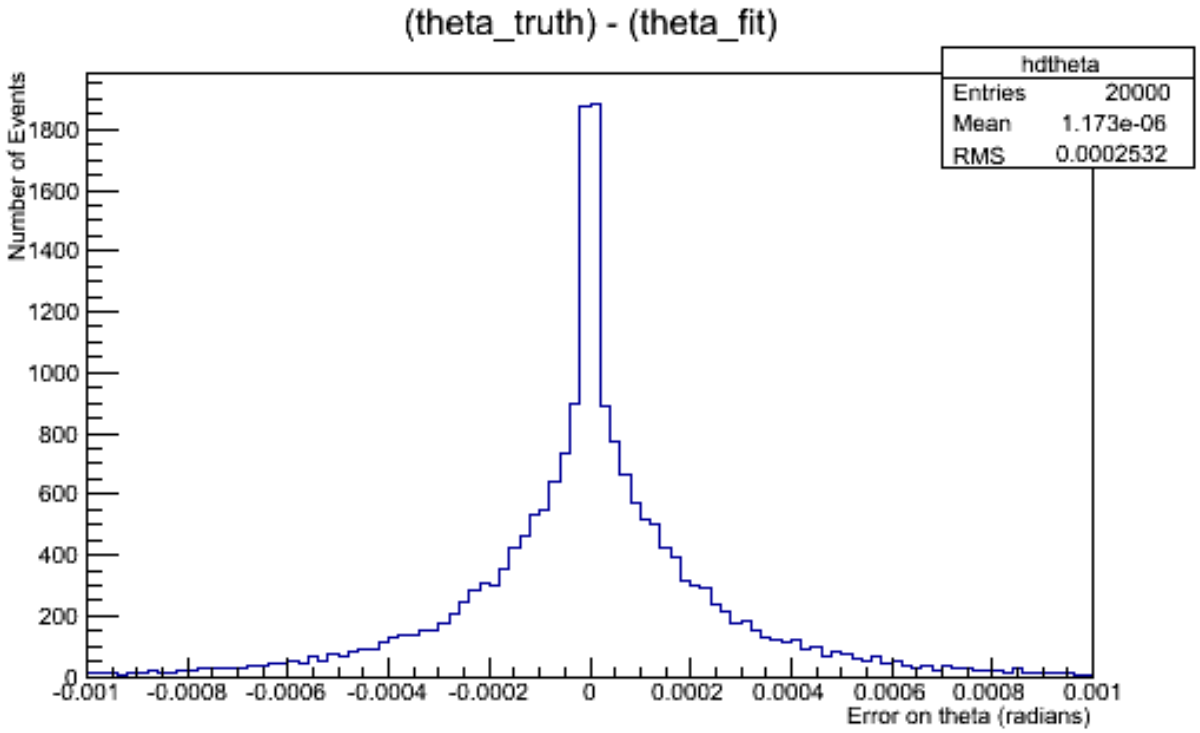

Figure 11: Resolution of theta for 8 hits

to that of the real inclination. This error can be seen in Figure 11, and it is clear that the error on θ is small, on the order of 10^{-6} radians.

5.5 Reconstruction Efficiency

Additionally, we looked at the effects of detector inefficiencies. Since detectors will only see muons with some probability, we changed how efficient individual detectors were to study the effects on resolution and efficiency. To study the efficiency, we studied how the efficiency of the detector changed the error on θ. As seen in Figure 18, detectors with 80% efficiency raise the error significantly. However, the efficiencies we expect are significantly higher and will not affect the error substantially. We also tried other constraints, such as a certain number of hits in each sector of detectors. Using these different requirements on how many detectors were fired, we could see the different effects on resolution, as defined before.

One final parameter that we varied was the alignment of the detectors. Ideally, the position of each detector is known perfectly, but unfortunately, detectors will shift and deform slightly, due to gravity, shifts in the ground, and basic inaccuracy in creating the detector. We did several studies on misaligned detectors, comparing the efficiencies of perfectly aligned detectors to setups with one detector per sector misaligned as well as those with four detectors shifted by the same amount. Figures 19 and 20 show the effects of these shifts on the error of θ. Shifting two individual detectors broadens the error while shifting entire sectors adds asymmetry to error, biasing whether the error will be positive or negative.

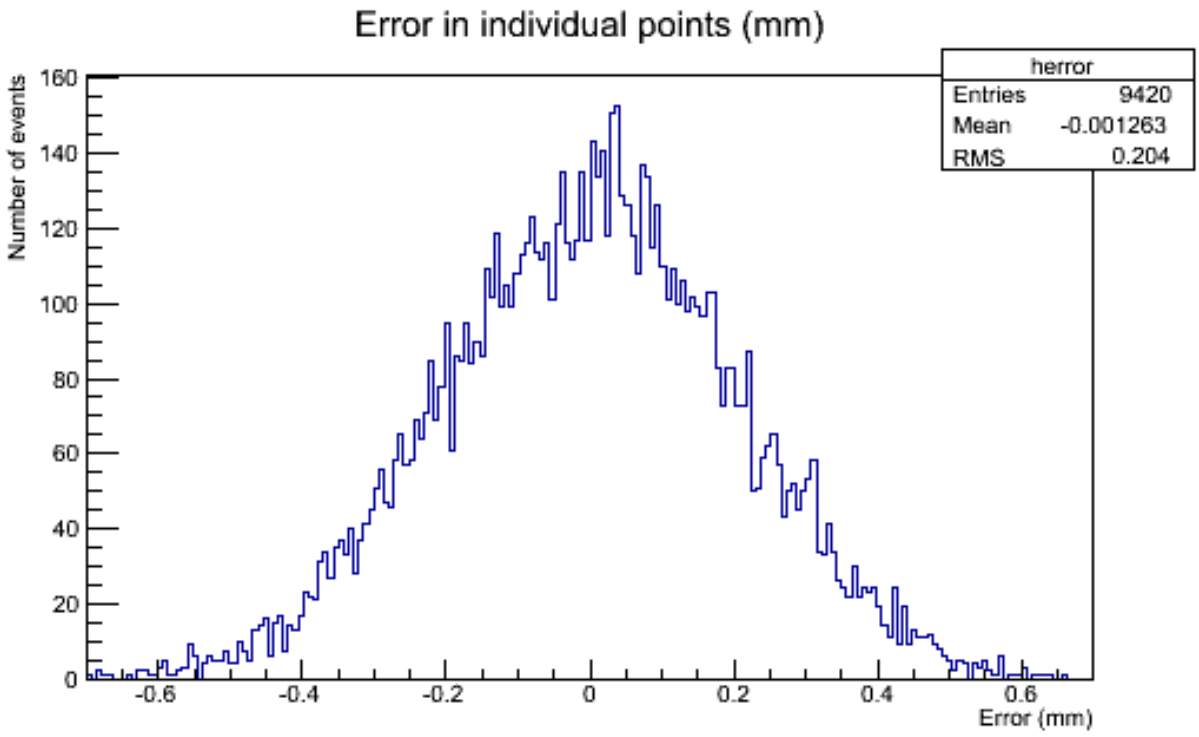

Figure 12: Resolution of hit location using single muon events

6 Conclusion

The upgrade of the ATLAS NSW is essential for new particle detection and precision measurements. The muon trigger system is particularly important in dereasing the fake rate and improving the resolution, so it is important to have a good understanding of the sTGC detectors. In these studies, we were able to model the proposed sTGC detectors for the ATLAS NSW. Our simulation of individual detectors gave a resolution consistent with test beam results. We were able to create an effective pattern detection algorithm which isolated the events from the muon hits, ignoring extra hits from delta-rays. Finally, we studied the detection efficiency and effects of misalignment on the resolution of the muon path. These studies indicate that the proposed sTGC detector satisfies the requirements for the NSW upgrade for high energy and high luminosity LHC runs.

7 Acknowledgments

Special thanks to Junjie for his support and guidance. Additional thanks to Robert and Katy for their motivation.

8 References

[1] ATLAS (2010). ATLAS Experiment Fact Sheet. Retrieved from ATLAS website: www.atlas.ch/fact-sheets-1-view.html

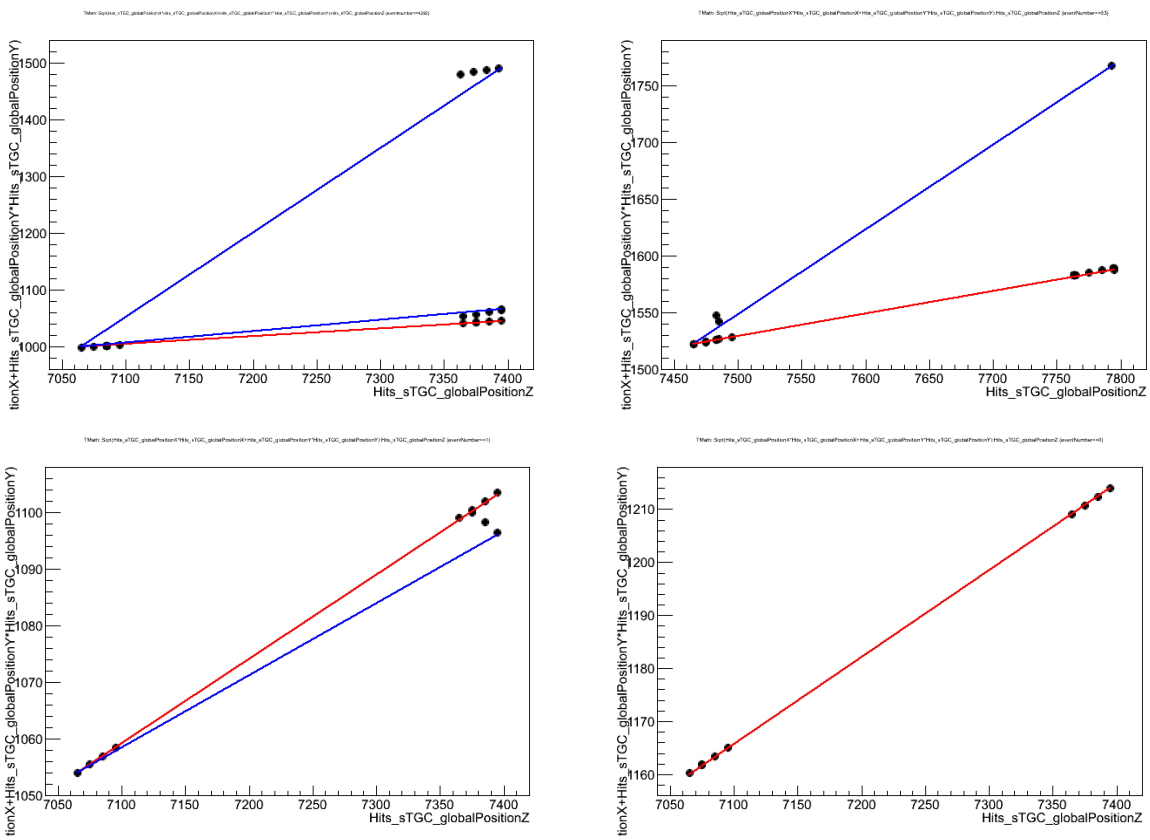

Figure 13: Example fitting of events. Red event is the one chosen.

[2] The ATLAS Collaboration (2008). The ATLAS Experiment at the CERN Large Hadron Collider. Journal of Instrumentation (3). iopscience.iop.org/1748-0221/3/08/S08003

[3] Han, T. (2005). Collider Phenomenology: Basic Knowledge and Techniques. arXiv: hep-ph/0508097

[4] Hoecker, A. (2009). Commissioning and early physics analysis with the ATLAS and CMS experiments. arXiv:1002.2891 [hep-ex]

[5] Roy, D.P. (1999). Basic Constituents of Matter and their Interactions – A Progress Report. arxiv.org/pdf/hep-ph/9912523v1.pdf

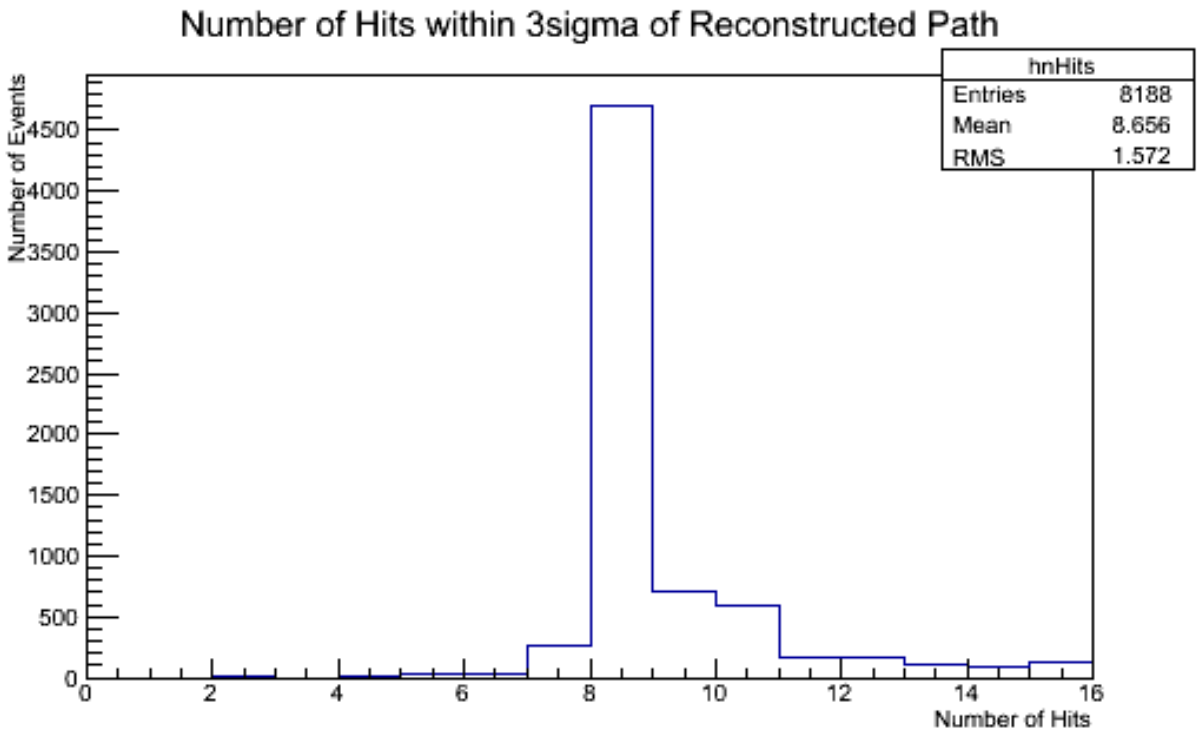

Figure 14: Number of Hits accepted per event

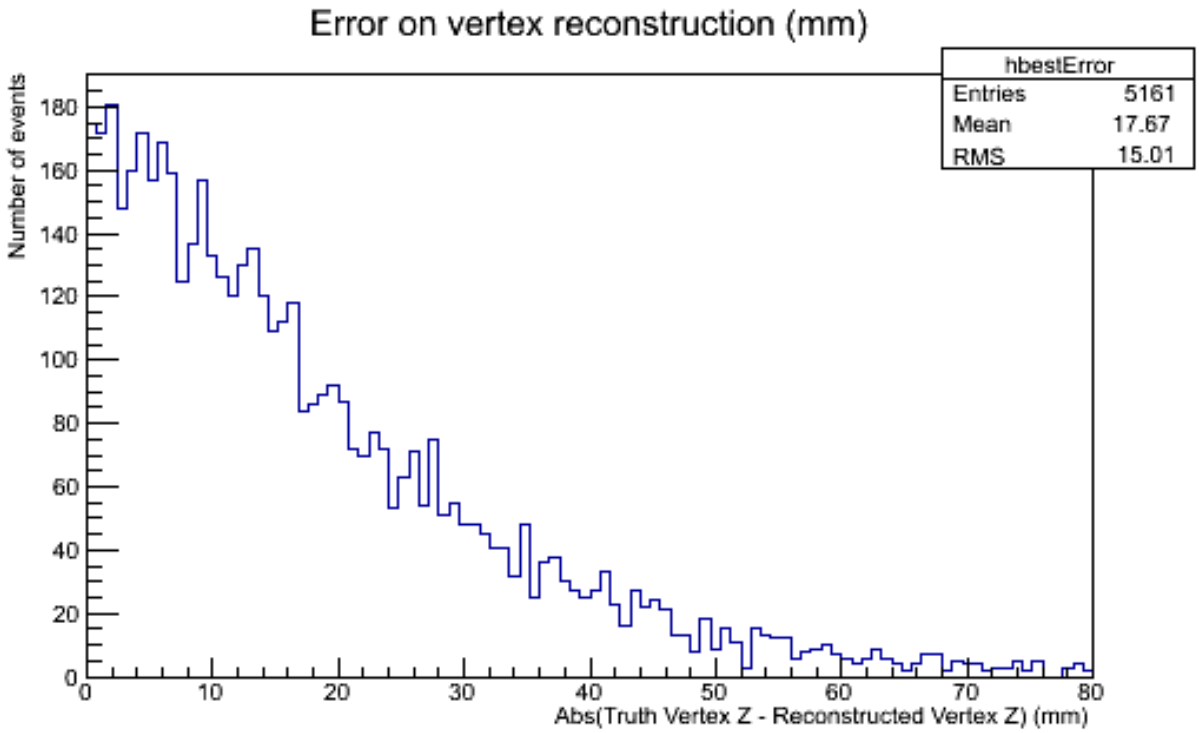

Figure 15: Difference between estimated and truth origin or muon (mm)

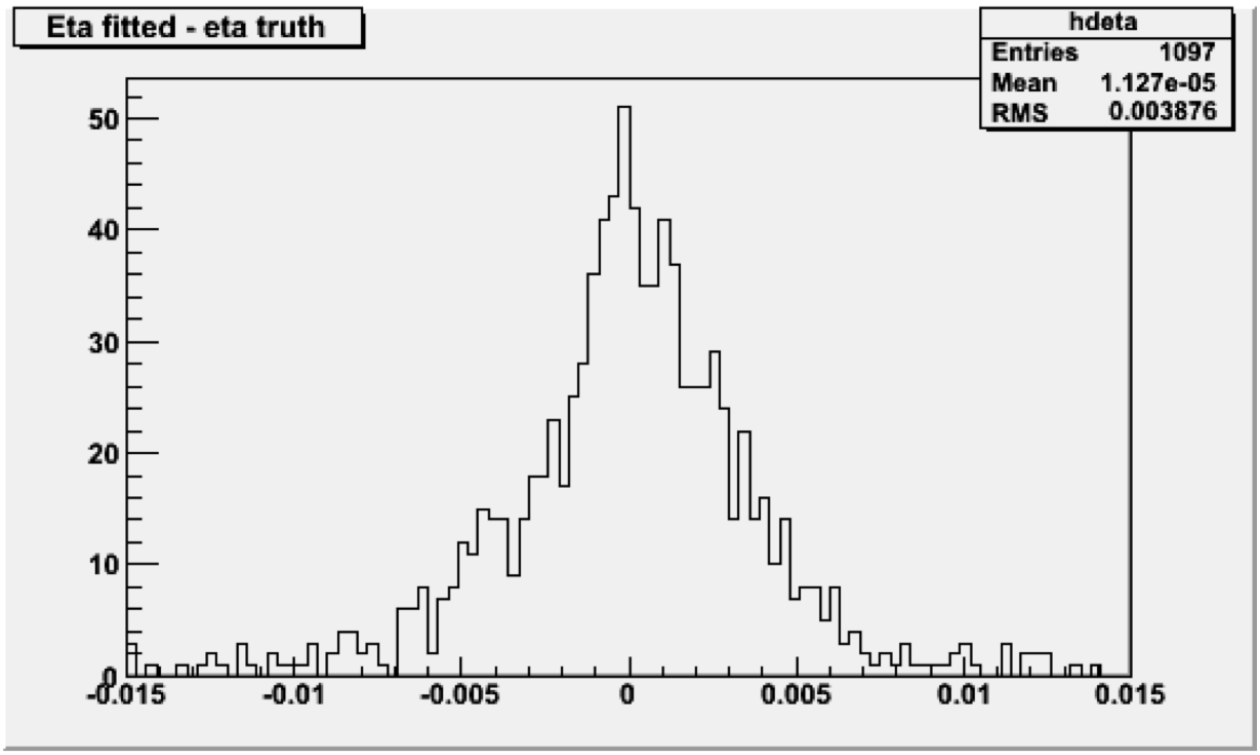

Figure 16: Resolution of eta measurement, calculated by the truth value of eta minus the calculated value.

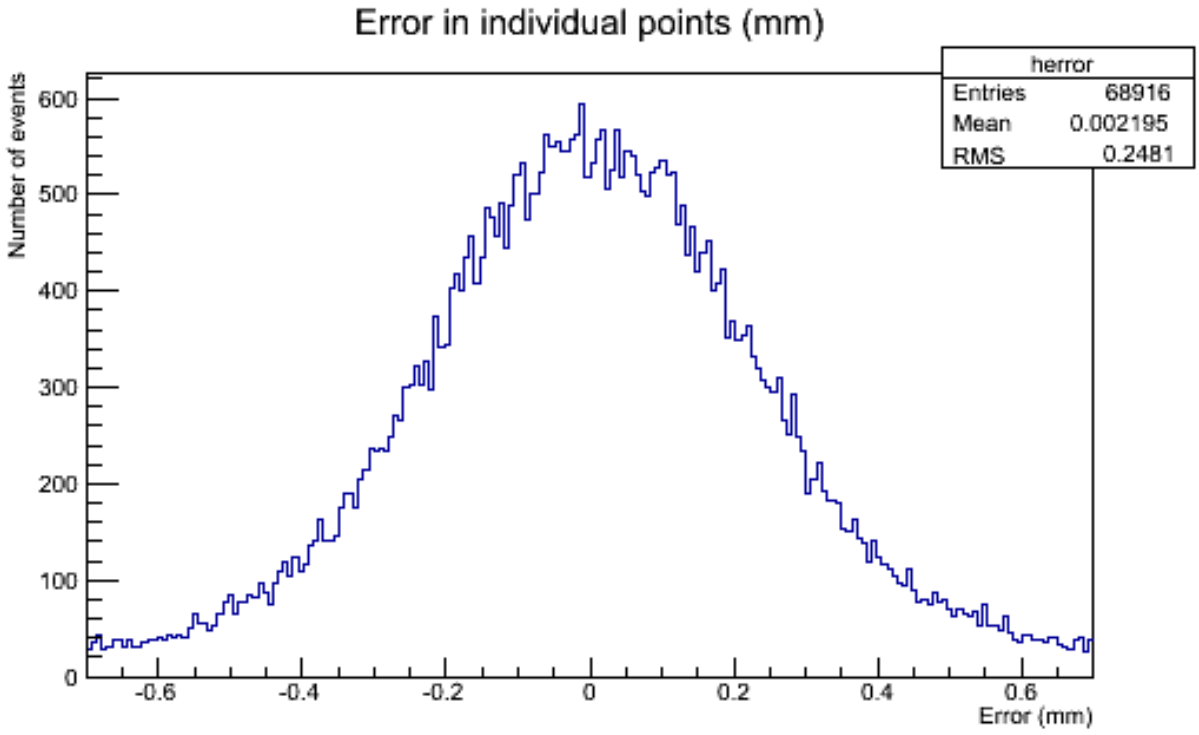

Figure 17: Deviations of hits from reconstructed line

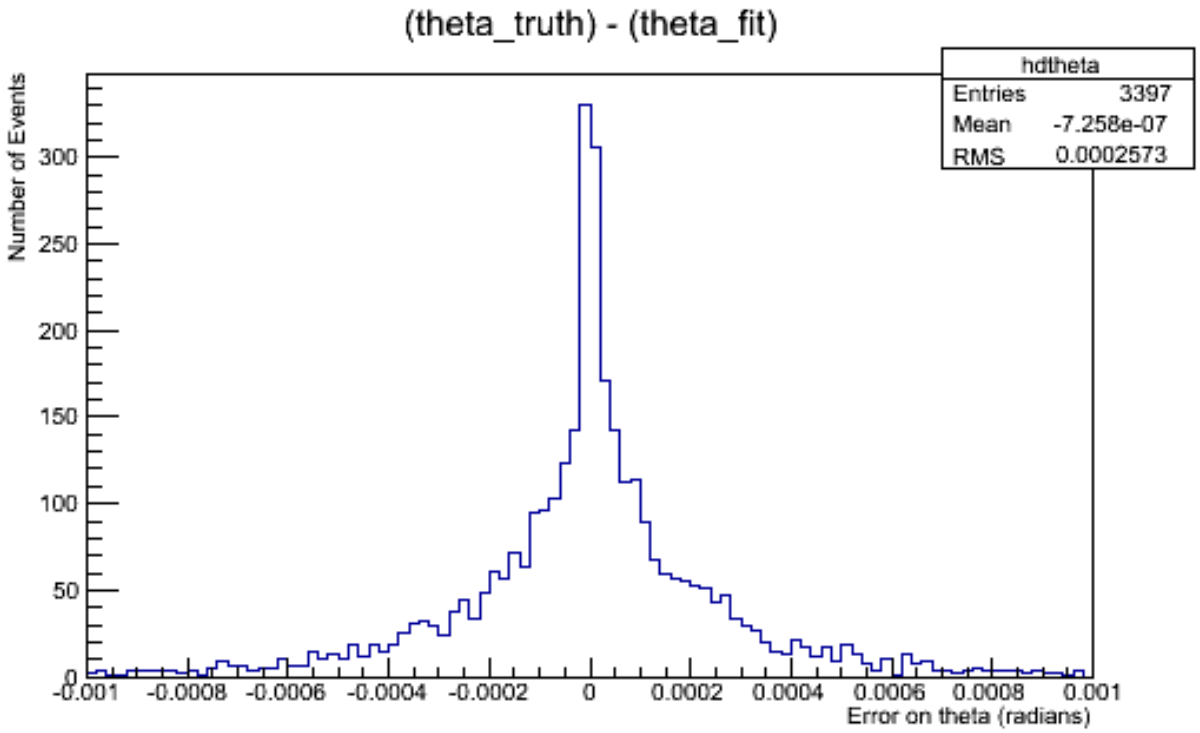

Figure 18: Resolution of θ using 80% efficient detectors

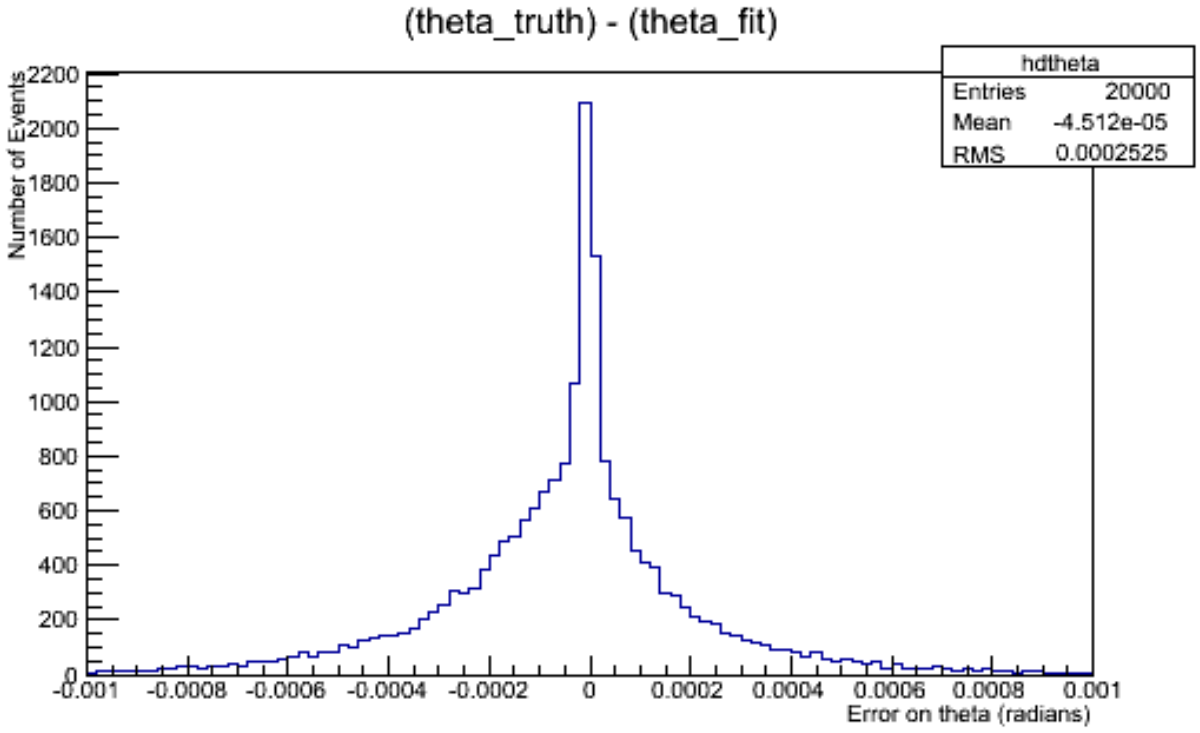

Figure 19: Resolution of θ with the 2nd and 7th detectors misaligned by -.05 and .05 mm respectively

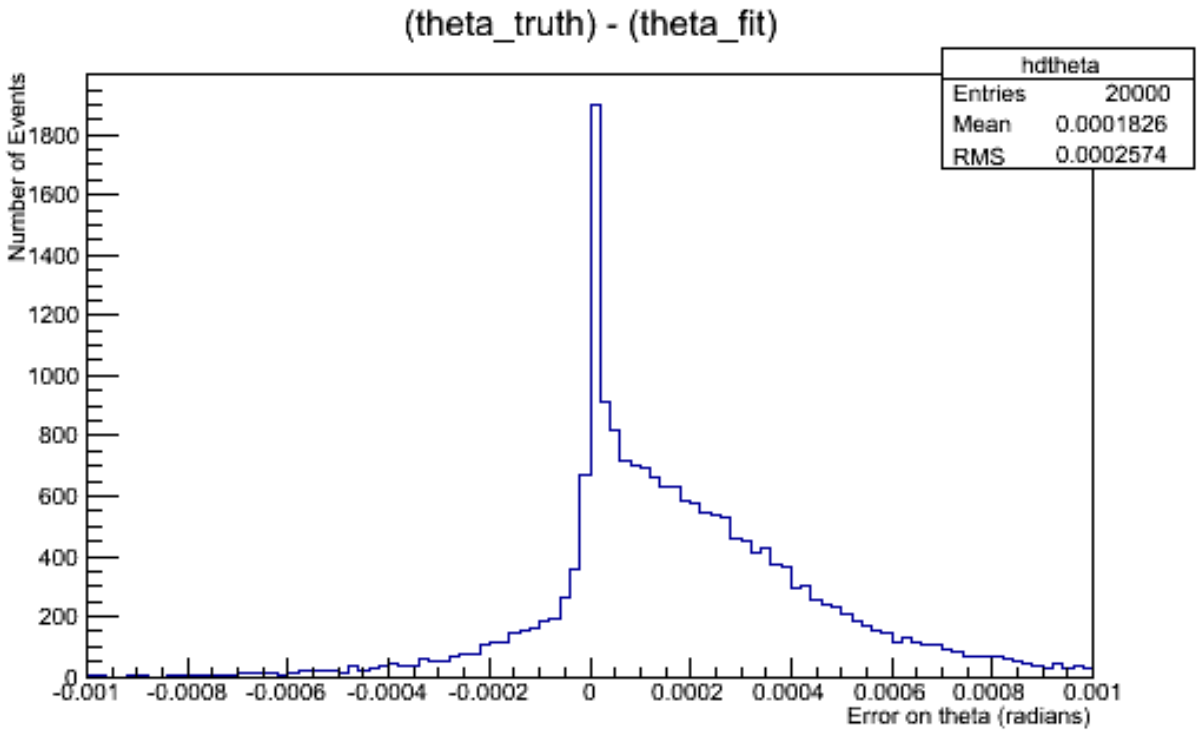

Figure 20: Resolution of θ with the first sector misaligned by .05 mm and the second by -.05 mm